

# Susceptibility and Magnetisation Measurements

Danny Bennett and Maeve Madigan

October 27, 2015

## Abstract

Using a Faraday balance, a Hall probe and an electronic balance, the magnetic susceptibility of the paramagnetic salt,  $\text{Gd}_3\text{Ga}_5\text{O}_{12}$ , was measured, and the hysteresis loop for the weakly ferromagnetic hematite- $\alpha\text{Fe}_2\text{O}_3$  was obtained, which was used to determine the spontaneous magnetisation, remanence, and coercivity of the material. The  $\vec{B}$ -field was calibrated and the nonlinear relationship between  $\vec{B}$  and  $I$  was observed, although a consistent choice of values of  $I$  eliminated the need to use a calibration curve. The field gradient was successfully calibrated; a value of  $C = (31.09 \pm 0.43) \text{ m}^{-1}$  was obtained for the calibration constant. This was then used to obtain a value of  $\chi = (0.6807 \pm 0.0007) \text{ J T}^{-2} \text{ kg}^{-1}$  for the magnetic susceptibility of  $\text{Gd}_3\text{Ga}_5\text{O}_{12}$ , which compared well to the expected value of  $\chi \approx 0.81 \text{ J T}^{-2} \text{ kg}^{-1}$  obtained using the Curie law. Hysteresis was successfully observed for hematite- $\alpha\text{Fe}_2\text{O}_3$ . From the graph, the saturation was estimated to be  $\sigma = 3653.55 \text{ J mT}^{-1}$ . Values of  $\sigma_s = 1450 \pm 186 \text{ J mT}^{-1}$  and  $B_c = 45 \pm 4 \text{ mT}$  were obtained for the remanence and coercivity, respectively, the low value of  $B_c$  being one possible explanation for the narrow hysteresis loop.

## 1 Introduction and Theory

The aims of this experiment were to calibrate the magnetic field by using a Hall probe to generate a  $\vec{B}(I)$  curve, to calibrate the field gradient using a sample of Mohr's salt ( $\chi \approx 0.33 \text{ J T}^{-2} \text{ kg}^{-1}$  at room temperature), to measure the susceptibility for a paramagnetic salt,  $\text{Gd}_3\text{Ga}_5\text{O}_{12}$ , and to plot the hysteresis loop of the ferromagnetic material, hematite- $\alpha\text{Fe}_2\text{O}_3$ .

### 1.1 Types of Magnetism

- **Paramagnetism:** In the absence of a magnetic field, the magnetic moments of a paramagnet are oriented randomly due to thermal fluctuations. When a magnetic field is applied, they begin to align parallel to the field and the magnetisation is proportional to the applied field:  $\vec{\sigma} = \chi \vec{B}$ . When the field is removed, thermal motion disrupts the magnetic alignment.
- **Ferromagnetism:** This occurs in some magnetic materials below the Curie temperature,  $T_C$ . Electron spins of atoms in microscopic regions (domains) are aligned. The magnetic field is strong in the domain, but since in the material the domains will be randomly ordered with respect to one another, it will usually be unmagnetised. In the presence of an applied magnetic field, the domains may line up with each other, causing the material to become magnetised. If the applied field is removed, the domains remain aligned, meaning ferromagnetic materials can exhibit spontaneous magnetisation (remanence): a net magnetic moment in the absence of an external magnetic field. Above the Curie temperature, the thermal motion is sufficient to disrupt the alignment, and the material becomes paramagnetic.
- **Antiferromagnetism:** The spins of magnetic electrons align in a pattern with adjacent spins pointing in opposite directions. There will therefore be no overall spontaneous magnetisation. This occurs below the Néel temperature,  $T_N$ , and above this temperature, the material becomes paramagnetic.

## 1.2 Faraday Balance

The magnetic moment of a magnet is a quantity that determines the torque it will experience in an external magnetic field. The energy associated with a magnetic dipole in a nonuniform magnetic field is given by

$$E = -\vec{m} \cdot \vec{B}, \quad (1)$$

where  $\vec{m}$  is its magnetic moment. Thus, the force is given by

$$\vec{F} = \vec{\nabla} (\vec{m} \cdot \vec{B}), \quad (2)$$

or

$$F_z = m_x \partial_z B_x + m_y \partial_z B_y + m_z \partial_z B_z, \quad \left( \partial_z = \frac{\partial}{\partial z} \right) \quad (3)$$

in component form. In the case of this experiment, the net magnetic moment of the sample points in the  $x$ -direction, but the field gradient produced by the curved inhomogeneous pole magnets points in the  $z$ -direction, so (3) reduces to

$$F_z = m_x \partial_z B_x. \quad (4)$$

If a magnetic sample is placed exactly in the middle of the pole magnets, it will experience a downward force in the  $z$ -direction. The magnetic moment of a sample,  $\vec{m}$ , is given by the product of magnetisation (per unit mass) and the mass,  $m$ , of the sample:

$$\vec{m} = m\vec{\sigma}. \quad (5)$$

The magnetisation of a paramagnet is given by

$$\vec{\sigma} = \chi \vec{B}, \quad (6)$$

where  $\chi$  is the magnetic susceptibility: a quantity which measures the response of the material to an applied magnetic field. Thus, for a paramagnet, (3) becomes

$$F_z = m\chi B_x \cdot \partial_z B_x. \quad (7)$$

A ferromagnet has a spontaneous magnetisation  $\sigma_s$  and hence a magnetic moment given by

$$\vec{m} = m\sigma_s \quad (8)$$

which is independent of the field applied when the atoms of the sample are aligned. When the magnetisation of a ferromagnet is saturated (when an increase in applied external magnetic field cannot increase the magnetization of the material further), (3) becomes

$$F_z = m\sigma_s \partial_z B_x. \quad (9)$$

The magnetic pole pieces are shaped such that the quantity  $(B_x^{-1} \cdot \partial_z B_x)$  is approximately constant over the length of the sample. Hence

$$F_z = Cm\chi B_x^2 \quad (10)$$

for a paramagnetic material. Therefore, the apparatus, known as the Farady balance, can be used to measure the magnetic susceptibility or magnetisation of a material. A current is used to create a nonuniform magnetic field between the two pole magnets. An electronic balance is used to measure the downward force on the sample, and after taking the weight of the sample into account, can be used to measure  $F_z$ , and hence  $\chi$  or  $\sigma_s$  can be determined.

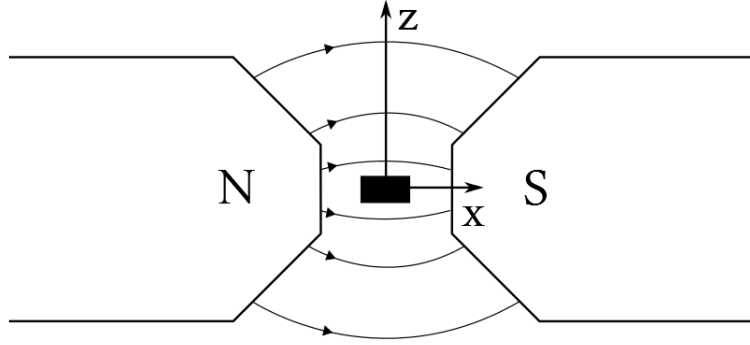


Figure 1: The Faraday balance.

### 1.3 Hysteresis

When a ferromagnetic material is magnetised in one direction, it will remain magnetised when the external field is removed. It can, however, be brought back to 0 with an external field in the opposite direction. If a ferromagnet is placed in an alternating magnetic field, its magnetisation,  $\sigma$ , as a function of field strength,  $H$ , should trace a closed loop. Initially, as the strength of the field is increased, the magnetisation increases and asymptotically approaches some value (magnetic saturation). When the field is decreased to 0 this time, the material will have a non-zero magnetisation (the remanence,  $\sigma_r$ ). The field is reversed, and then increased until the magnetisation reaches 0 again. The strength of the field that this occurs at is known as the coercivity,  $B_c$ , of the ferromagnet. After repeating this process, the loop that is traced out is known as the hysteresis loop.

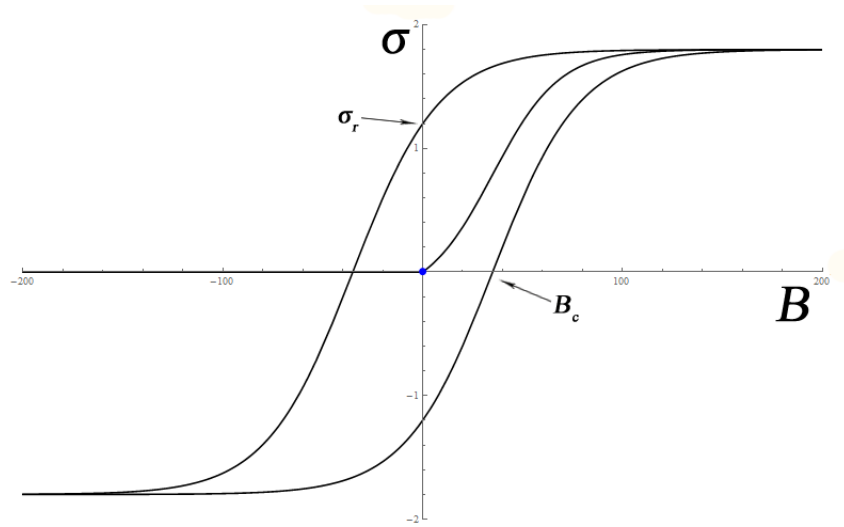


Figure 2: The hysteresis loop of a ferromagnetic material.

## 1.4 The Curie Law

The Curie law states that in a paramagnetic material, the magnetisation is (approximately) directly proportional to an applied magnetic field, and inversely proportional to the temperature:

$$\vec{\sigma} = C \frac{\vec{B}}{T}. \quad (11)$$

$C$  is the Curie constant, given by

$$C = \frac{\mu_B^2}{3k_B} N g^2 J(J+1), \quad (12)$$

where  $\mu_B$  is the Bohr magneton,  $k_B$  is the Boltzmann constant,  $J$  is the quantum number,  $N$  is the number of magnetic ions per kg, and  $g$  is the Landé  $g$ -factor. From (6) it follows that

$$\chi = \frac{\mu_B^2}{3k_B T} N g^2 J(J+1), \quad (13)$$

and using this, the expected susceptibility of a paramagnetic material can be determined.

## 2 Experimental Method

### 2.1 Apparatus

The apparatus used in the experiment is similar to the setup of the Faraday balance. Two solenoids are placed around the curved magnets, and a current (varied by a potentiometer) can be ran through them in order to generate the magnetic field. The direction of the current can be changed to change the polarity of the magnetic field. A holder, connected to an electronic balance, hangs from above, midway between the curved magnets. Magnetic samples can be placed in the holder, and their properties can be investigated. A Hall probe which is connected to a Gaussmeter is used to initially calibrate the  $\vec{B}$ -field meaning that in the proceeding parts of the experiment, the value of the current can be quickly converted into a value for  $\vec{B}$ , rather than having to measure the  $\vec{B}$ -field each time. The electronic balance was very sensitive (accurate to  $10^{-7}$  kg), and therefore caution is needed in the vicinity so as not to disrupt any series of measurements. Another factor which must be taken into consideration is the mass of the sample used. If the mass is too large, then the force in the  $x$ -direction will be of the same order of magnitude as the force in the  $z$ -direction, and as the current is increased, it will be pulled towards one of the magnets, disrupting the experiment. If the mass of the sample is too small, the force in the  $z$ -direction will be negligible, leading to inaccurate results. Thus, an adequate mass of the sample must be determined in each case before continuing with the experiment.

### 2.2 Procedure

For the first part of the experiment, the  $\vec{B}$ -field at the position of the sample was calibrated. The sample holder was removed and the Hall probe was aligned with the position the sample holder would be in. The apparatus was correctly switched on and the value of the  $\vec{B}$ -field was recorded from the Gaussmeter. The current was varied by the potentiometer and a series of values for  $B_x$  as a function of  $I$ , the current, were taken. The current was then brought back to 0, the direction of the current was reversed, and a series of values in the  $-x$ -direction were taken. These values were plotted and the relationship between  $\vec{B}$  and  $I$  was observed. This also allowed for the values of  $I$  to be easily converted into their corresponding values of  $B_x$  in later parts of the experiment.

For the second part of the experiment, the field gradient was calibrated so that the susceptibility of a paramagnetic material could then be measured. A mass of Mohr's salt, the susceptibility of which was known ( $\chi \approx 0.33 \text{ J T}^{-2} \text{ kg}^{-1}$  at room temperature), was used to accomplish this. The apparent mass of the Mohr's

salt was determined, and then a series of values of  $F_z$  vs  $I$  (and hence  $B_x$ ) were obtained. By using (10) and plotting  $F_z$  vs  $B_x^2$ , the value of  $C$  can be determined using the slope of this graph, since the mass of the sample and the susceptibility are known. For the third part of the experiment, the magnetic susceptibility of  $\text{Gd}_3\text{Ga}_5\text{O}_{12}$  was determined. A series of values of  $F_z$  vs  $B_x^2$  were plotted and the slope of this graph was used to determine the susceptibility, since  $m$  and now  $C$  are known. This value of  $\chi$  was compared to the expected value obtained from (13).

For the fourth part of the experiment, the magnetisation of the weakly ferromagnetic material hematite- $\alpha\text{Fe}_2\text{O}_3$  was investigated. By taking a series of values of  $F_z$  for values of  $B_x$  and using (9), the dependence of  $\sigma$  on  $\vec{B}$  can be determined. When the magnetisation approaches saturation, the  $\vec{B}$ -field is reversed and when  $\vec{B}$  is brought to 0, the magnetisation should be nonzero. At this point, the polarity of  $\vec{B}$  is reversed and the process is repeated. By reversing the polarity of  $\vec{B}$  once more, the hysteresis loop should be completed. Values for the remanence, coercivity and saturation can be determined from this, and the fact that the magnetisation of a ferromagnetic material depends on its past can be observed.

### 3 Results and Analysis

#### 3.1 Error Analysis

Using the general formula

$$\frac{\Delta f(x, y)}{f(x, y)} = \sqrt{\left(\frac{\Delta x}{x}\right)^2 + \left(\frac{\Delta y}{y}\right)^2}, \quad (14)$$

the uncertainty in the calibration constant,  $C$ , was determined. The value of  $\chi$  was taken to be  $0.33\text{J T}^{-2}\text{kg}^{-1}$ , the uncertainty in the mass of the Mohr's salt was  $\Delta m_M = 0.0001\text{g}$ , and the uncertainty in the slope was  $\Delta M = 0.04 \times 10^{-10}\text{N m T}^{-2}$ , which lead to a value of  $\Delta C = 0.43$  for the uncertainty in  $C$ . A similar method was used to determine the error in the susceptibility of  $\text{Gd}_3\text{Ga}_5\text{O}_{12}$ ; the error in the slope of the line was  $\Delta M = 4 \times 10^{-12}\text{N m T}^{-2}$ , and the error in the mass of the sample was the same as before. This lead to an uncertainty of  $\Delta\chi = 0.0007\text{J T}^{-2}\text{kg}^{-1}$ .

To obtain the uncertainty  $\Delta B_x^2$ , the general formula

$$\Delta f(x) = \frac{\partial f}{\partial x} \Delta x \quad (15)$$

was used. Thus, the uncertainty  $\Delta B_x^2$  was given by

$$\Delta B_x^2 = 2B_x \Delta B_x. \quad (16)$$

The values of  $B_x$  were measured to either  $0.1\text{mT}$  or  $1\text{mT}$  depending on the magnitude. The corresponding  $\Delta B_x^2$  was determined in each case.

#### 3.2 Results

In the first part of the experiment,  $I$  was varied and the resulting value of  $B_x$  was recorded in each case. This was done for both positive and negative values of  $B_x$ . The data is plotted and is shown below. It was possible to fit a nonlinear curve through the data points, and then for any value of  $I$  (within the range of the graph), the corresponding value of  $B_x$  could be found. However, a more convinient method was to choose a consistent set of values of  $I$  throughout the experiment and hence use the same values of  $B_x$  in each case, as the empirical fit was a polynomial of degree 9. In any case, the nonlinear relationship between  $B_x$  and  $I$  was observed.

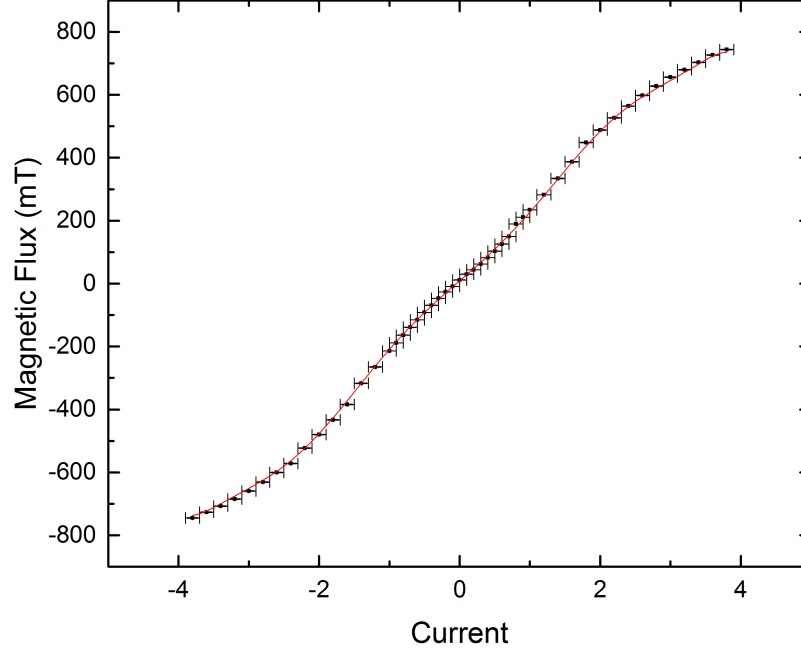


Figure 3: Calibration of the  $\vec{B}$ -field. The negative values of  $I$  mean that the current was changed to flow in the opposite direction.

In the second part of the experiment, the mass of Mohr's salt used was  $m_M = 0.0944\text{g}$ . A series of values of  $F_z$  and  $B_x^2$  were taken, and a straight line was fitted through the data points. The slope of the graph was  $M = (9.67 \pm 0.04) \times 10^{-10} \text{N mT}^{-2}$ . For the sample of Mohr's salt, the susceptibility was taken to be  $\chi = 0.33$ . Using

$$C = \frac{M}{m_M \chi}, \quad (17)$$

a value of  $C = (31.09 \pm 0.43) \text{m}^{-1}$  for the calibration constant.

Having found this calibration constant, the magnetic susceptibility of  $\text{Gd}_3\text{Ga}_5\text{O}_{12}$  was determined. A series of values of  $F_z$  vs  $B_x^2$  were plotted, and a linear fit was obtained. The slope of the line was  $M = (1.405 \pm 0.004) \times 10^{-9} \text{N mT}^{-2}$ . Using a similar formula to (17), the value obtained for the magnetic susceptibility of  $\text{Gd}_3\text{Ga}_5\text{O}_{12}$  was  $\chi = (0.6807 \pm 0.0007) \text{J T}^{-2} \text{kg}^{-1}$ . To calculate the expected value  $\chi$ ,  $N = 3N_A$ , where  $N_A$  is Avagadro's number, since the only magnetic ion in  $\text{Gd}_3\text{Ga}_5\text{O}_{12}$  is  $\text{Gd}^{3+}$  and there are 3 moles of it,  $g = 2$  and  $J = \frac{7}{2}$ . Using (13), an expected value of  $\chi \approx 0.81 \text{J T}^{-2} \text{kg}^{-1}$  was obtained.

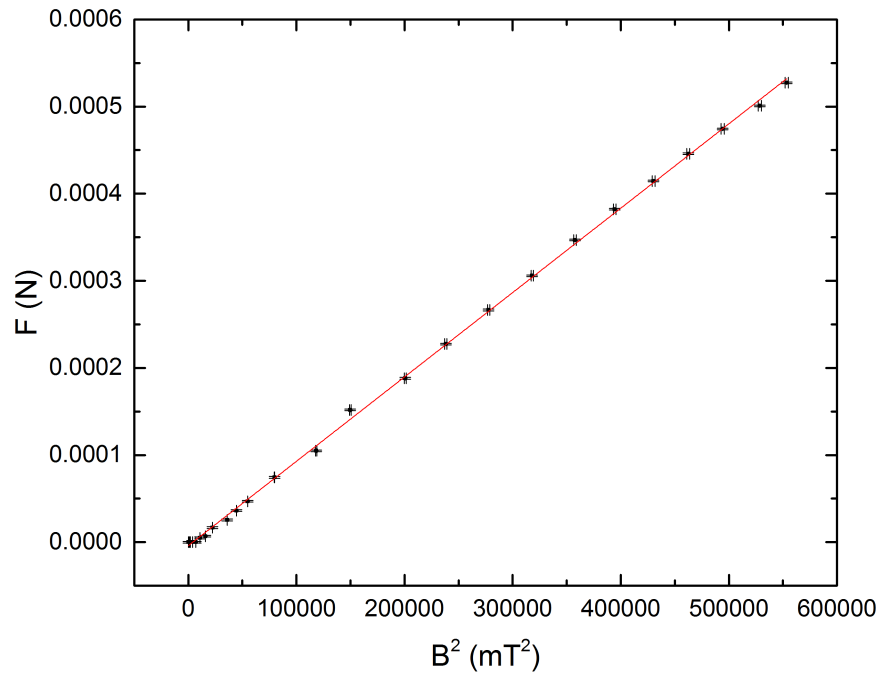


Figure 4: Calibration of the  $\vec{B}$ -field gradient.

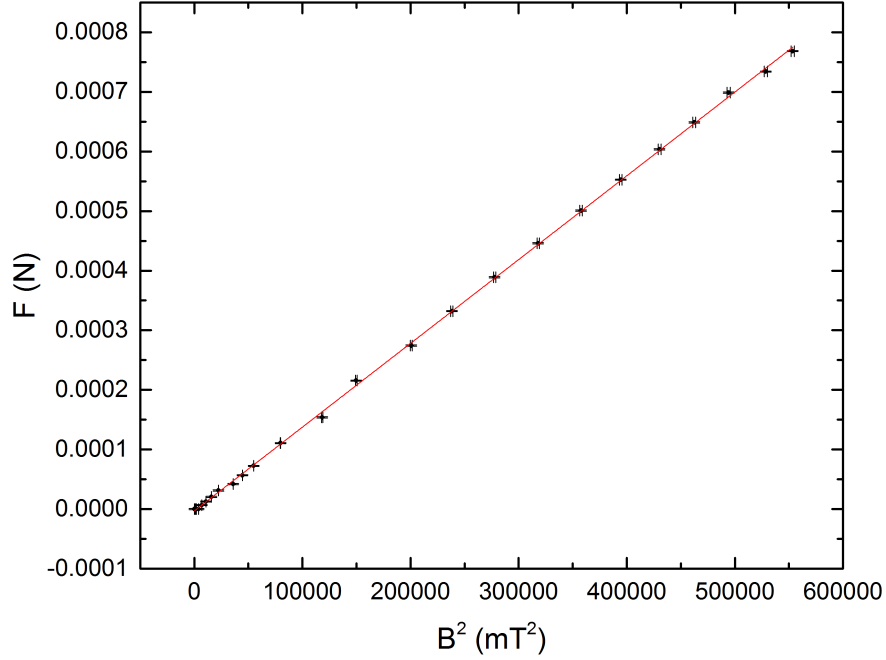


Figure 5: Determination of  $\chi$  for the paramagnetic salt.

Values of  $F_z$  were obtained for corresponding values of  $B_x$  until saturation was achieved. The  $\vec{B}$ -field was then decreased again, and at 0 the direction was reversed and the process was repeated. The direction of the  $\vec{B}$ -field was increased again. Values of  $\sigma$  were obtained from the values of  $F_z$  using (9), and the hysteresis loop for hematite- $\alpha\text{Fe}_2\text{O}_3$  was successfully plotted and is shown below, although it is quite a narrow loop and in some parts of the graph it is difficult to distinguish the behaviour of the material. From the graph, values of  $\sigma$ , the saturation were estimated from the asymptotic parts of the graph, both upper and lower, and an average value was taken. Values of  $\sigma = 3261.85\text{J mT}^{-1}$  and  $\sigma = -3685.25\text{J mT}^{-1}$  were estimated for the upper and lower parts of the graph, so an average value of  $\sigma_s = 3653.55\text{J mT}^{-1}$  was estimated for the saturation of hematite- $\alpha\text{Fe}_2\text{O}_3$ . Values of  $\sigma_r = 1450 \pm 186\text{J mT}^{-1}$  and  $B_c = 45 \pm 4\text{mT}$  were obtained for the remanence and the coercivity.

## 4 Discussion and Conclusions

The nonlinear relationship between the current and magnetic field was observed, and thus the magnetic field was successfully calibrated. It was possible to fit a nonlinear curve through the data points, and was technically possible to determine  $B_x$  for any value of  $I$ , but this was inconvenient as the curve was a polynomial of degree 9. Instead, this process was avoided by a convenient choice of values of  $I$  with the potentiometer; the same set of values were used in future parts of the experiment.

The field gradient was successfully calibrated by using the Mohr's salt. A value of  $C = (31.09 \pm 0.43)\text{m}^{-1}$  was obtained for the calibration constant. The dimensions of  $C$  were determined using dimensional analysis. There was no expected value which the obtained value of  $C$  could have been prepared to, although the comparison of the obtained value for the susceptibility for  $\text{Gd}_3\text{Ga}_5\text{O}_{12}$  with the expected value is a good



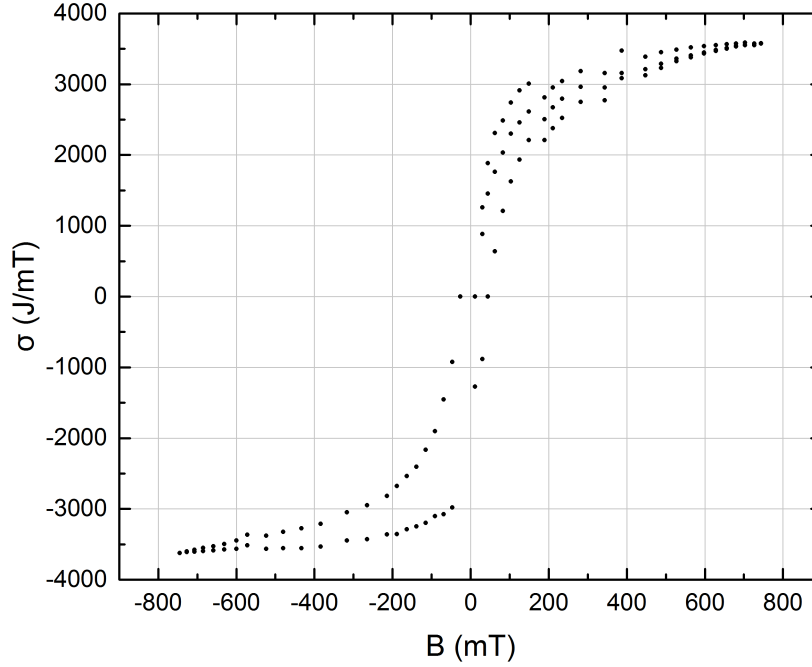


Figure 6: The hysteresis loop for hematite- $\alpha\text{Fe}_2\text{O}_3$ .

indicator to the accuracy of the calibration constant.

A value of  $\chi = (0.6807 \pm 0.0007) \text{ J T}^{-2} \text{ kg}^{-1}$  was obtained for the magnetic susceptibility of  $\text{Gd}_3\text{Ga}_5\text{O}_{12}$ . This compares well to the expected value that was obtained using the Curie law, which was  $\chi \approx 0.81 \text{ J T}^{-2} \text{ kg}^{-1}$ . The obtained value is not correct within the range of error and uncertainty, but it is quite small in comparison to the susceptibility itself. One possible reason for this is that the electronic balance is very small and therefore has a small uncertainty associated with it. Another possibility is that an error in calculation was made when determining  $\Delta\chi$ . One source of error was determining the correct amount of the material to use. If the mass is too large, the force on the material in the  $x$ -direction disrupts the experiment. If it is too small, the initial values for  $F_z$  are negligible when compared to the larger ones. In this experiment, the mass used was too small, as the initial values for  $F_z$  in these cases were taken to be 0, as the magnitudes of the masses were lower than the precision of the electronic balance.

The hysteresis loop for hematite- $\alpha\text{Fe}_2\text{O}_3$  was successfully observed. An average value of  $\sigma = 3653.55 \text{ J mT}^{-1}$  was estimated for the saturation of hematite- $\alpha\text{Fe}_2\text{O}_3$ , and values of  $\sigma_r = 1450 \pm 186 \text{ J mT}^{-1}$  and  $B_c = 45 \pm 4 \text{ mT}$  were obtained for the remanence and the coercivity. The value for  $B_c$  is quite small, which would explain why the hysteresis loop is very narrow. It would be impossible to obtain a perfect hysteresis loop in this setting because ferromagnetic materials can become permanently magnetised, and it is possible that the hematite- $\alpha\text{Fe}_2\text{O}_3$  was still magnetised from the previous experiment.

## 5 Appendix

Shown below are the equations of the curves that were fit through the data points in each part of the experiment.

Model	Poly		
Equation	$y = a_0 + a_1x + a_2x^2 + a_3x^3 + a_4x^4 + a_5x^5 + a_6x^6 + a_7x^7 + a_8x^8 + a_9x^9;$		
Reduced Chi-Sqr	7409.88745		
Adj. R-Square	0.99365		
		Value	Standard Error
Magnetic Flux	a0	8.27648	1.04937
	a1	194.44107	5.98898
	a2	1.0832	6.11649
	a3	29.72128	10.05896
	a4	-0.98513	4.74014
	a5	-6.22189	3.44571
	a6	0.11551	0.74206
	a7	0.46329	0.40399
	a8	-0.00384	0.03134
	a9	-0.01213	0.01479

Figure 7: Calibration of the  $\vec{B}$ -field.

Equation	$y = a + b \cdot x$		
Weight	Instrumental		
Residual Sum of Squares	400.90635		
Pearson's r	0.99978		
Adj. R-Square	0.99953		
		Value	Standard Error
F	Intercept	-4.0852E-6	1.15935E-6
	Slope	9.68509E-10	4.27603E-12

Figure 8: Calibration of the  $\vec{B}$ -field gradient.

Equation	$y = a + b \cdot x$		
Weight	Instrumental		
Residual Sum of Squares	411.25685		
Pearson's r	0.99989		
Adj. R-Square	0.99977		
		Value	Standard Error
F	Intercept	-3.03366E-6	1.17422E-6
	Slope	1.40532E-9	4.33088E-12

Figure 9: Determination of  $\chi$  for the paramagnetic salt.

## References

- [1] John MD Coey. Magnetism and magnetic materials. Cambridge University Press, 2010.
- [2] John R Hook and Henry Edgar Hall. Solid state physics (the manchester physics series), 2000.